The effects of composition and thermal path on hot ductility of forging steels

B. M. Connolly, J. Paules, A. DeArdo

This work examines the effects of composition and thermal handling path on the hot ductility of as-cast steel forging ingots. Poor ductility of the as-cast structure can lead to cracking of the ingot prior to forging or the formation of tears early during the forging process. The as-cast structure is particularly susceptible to cracking due to the large grain size and high degree of microsegregation present.

Experiments were conducted to evaluate the ductility of the as-cast steel with varying levels aluminum and nitrogen. Multiple thermal handling paths were followed in order to approximate the different thermal conditions experienced approximately six inches below the surface of a large (~40 MT) steel ingot following solidification. Hot tension testing after in-situ melting and solidification was used for quantitative measurements of the material ductility. The majority of testing was carried out on a modified P20 mild tool steel. The experiments indicate a significant loss of ductility for materials with high aluminum and nitrogen contents (AlxN = 5.2x10^{-4}) in the temperature range of 950 °C - 1050 °C upon solidification and direct cooling to the test temperature. This behavior is not present in material with AlxN products below 1.3x10^{-4}. All materials tested exhibited a loss of ductility when the sample was cooled to 900 °C, immediately reheated to 1000°C and tested. With increasing hold times at 900 °C prior to reheating to 1000 °C, the material with high aluminum and nitrogen contents recovers ductility much more quickly than the low aluminum and nitrogen materials.

Funding in part by the Forging Industry Educational & Research Foundation and Ellwood Group, Inc.

Keywords: Steel - Hot Ductility - Aluminum Nitride

INTRODUCTION

Steel ingots remain a leading raw material for forging facilities producing critical large cross-section parts in the energy, mining, defense and aerospace industries. Since the 1960's, continuous casting has largely replaced ingot casting due to increased yields and an improved as-cast structure.

However, continuous casting is currently limited in cross-section to approximately 800 mm diameter maximum which precludes the material from use in heavy section products. Steel ingots can be cast in weights up to 600 MT and cross sections up to 4.2 meters. Steel ingots are also frequently used for specialty steel grades that are not conducive to continuous casting due to either the chemical composition or low tonnage requirements.

Steel ingots of various compositions can experience poor hot ductility that leads to cracking which becomes apparent during the forging process. Hot ductility troughs have been identified and analyzed by many researchers [2, 3, 4, 5] in the temperature range of 700° - 1200°C, with the exact temperature range and severity of the trough varying by investigator, composition and experimental conditions. The ductility trough is often depicted by plotting hot tension percent reduction of area at failure (%RA) against test temperature for multiple samples. A rapid drop in %RA values is commonly shown within the temperature range noted above, while ductility is higher both above and below the trough. This loss in ductility has been attributed to many factors including precipitation of nitrides and/or carbides, segregation of impurities to austenitic grain boundaries, formation of ferrite at austenitic grain boundaries and combinations of these with other factors. At lower temperatures, well below the Ar_3 temperature, the ductility usually returns to high %RA values. At higher temperatures ductility is recovered by increased grain boundary mobility, dissolution and/or coarsening of

Brendan M. Connolly
Ellwood Quality Steels and University of Pittsburgh
John Paules
Ellwood Material Technologies
Dr. Anthony DeArdo
University of Pittsburgh
Paper presented at the 2nd Int. Conf. Ingot Casting Rolling and Forging - ICRF 2014, Milan 7-9 May 2014

Steel	C	Mn	P	S	Si	Ni	Cr	Mo	V	Cu	Al	N	AlxN ($x10^4$)
P20-low	.34	1.45	.013	.003	.29	.80	1.97	.22	.057	.19	.0075	.0081	.6075
P20-mid	.34	1.46	.008	.002	.30	.81	1.99	.22	.055	.17	.015	.0085	1.275
P20-high	.34	1.53	.011	.003	.34	.78	2.03	.22	.059	.19	.040	.0130	5.200
3.5Ni	.34	.73	.006	.002	.20	3.52	.99	.60	.061	.15	.012	.0073	.8760
4130	.33	.55	.007	.001	.32	.14	1.04	.22	.048	.17	.015	.0099	1.485

Table 1: Compositions of steels examined (wt %)

grain boundary precipitates and an increased ability to recrystallize. At temperatures approaching the solidus, ductility drops sharply due to incipient melting.

EXPERIMENTAL WORK

Commercial heats of the desired compositions (see Table 1, compositions in wt %) were produced.
The P20 material is a mild tool steel and heats were produced with varied (low/mid/high) aluminum and nitrogen contents. The 3.5Ni and 4130 materials were produced with aluminum and nitrogen contents as close as possible to those of the P20-mid material.
Steel samples were provided by Ellwood Group, Inc. from slices of forged ingots. No samples were taken within 150 mm of the metallurgical centerline of the slices in order to avoid compositional variations due to macrosegregation, namely for carbon and sulfur.
Hot ductility can be tested by several methods [6] including hot torsion, compression, tension and bending. Hot tension is the testing method in this work due to the quantitative nature of the ductility measurement. In a manner outlined by Revaux, Bricout and Oudin [2], in-situ solidification may be performed within the tension testing apparatus. In-situ cast specimens exhibit grain boundary segregation of aluminum which may reduce the bulk concentrations required to exceed the solubility limit for AlN formation [11], as is the case for as-cast forging ingots.
In-situ solidification can introduce a shrinkage cavity into the sample due to the volume contraction that occurs during the liquid to austenite phase transformation. The design of the crucible in the present work maintains soundness in the deformation zone by using a big-end-up taper of ~7% and by introducing a notch at the mid-height of the crucible. The notched area, with the smallest cross-section, will bear the strain. The solidification cavity remains above the notched area because as solidification progresses, the higher density solid crystallites tend to fall through the liquid allowing a progression of the solidified front from bottom to top. Revaux, Bricout and Oudin used light pressure to ensure the solidification cavity was moved outside of the deformation zone; the same method was employed in the current work. Only slight modifications were made to the sample configuration, and the design of the fused quartz crucible is nearly identical to that used by Revaux, Bricout and Oudin. The sample and crucible dimensions for this work are shown in Figure 1.

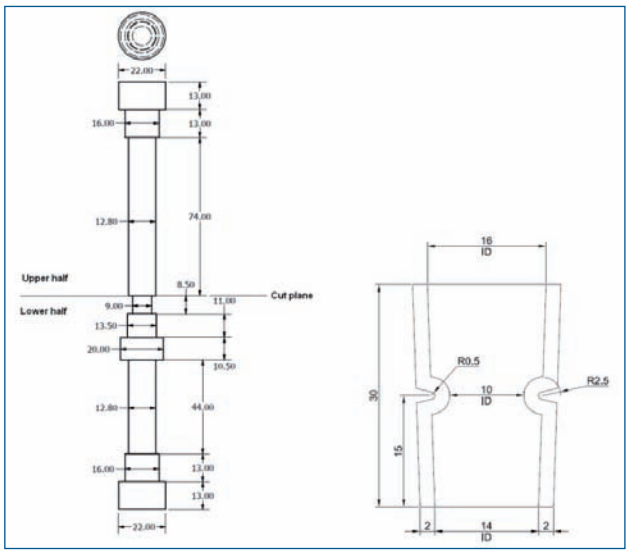

Fig. 1 - Sample and crucible dimensions for this work

EQUIPMENT

An Instron testing frame was fitted with high-temperature alloy grips, insulated heating chamber and inert gas purging. The heating chamber was constructed from a 10” diameter steel cylinder with 1/8” wall thickness. The cylinder is insulated with 1” thick refractory fiber and has a 4”x4” high temperature glass viewing window for observation during testing. The cylinder is fixed to the upper tensile grip arm and is hinged along its vertical axis for sample access. The heating chamber has ports for inert gas purging, induction coil, optical pyrometer sight and an access port for breaking the melt crucible away from the sample. A rendering of the insulated heating chamber mounted on the tensile frame is shown below in Figures 2a and 2b.
The three-turn water-cooled induction coil is connected to a 10 kW Pillar MK-20 computer controlled power supply. The induction coil leads are isolated from the heating chamber shell using electrically insulating cloth. Temperature readings are obtained from an Omega IR2C dual color optical pyrometer at a rate of $1s^{-1}$.

TESTING

The tensile sample halves are placed into the grips with

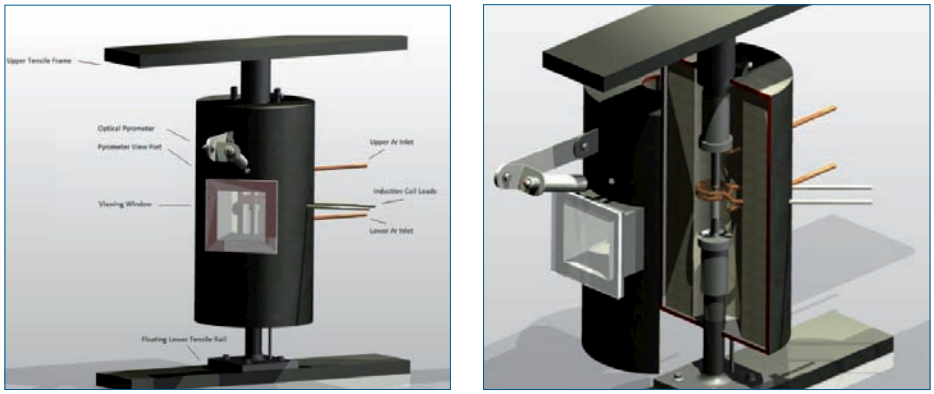

Fig. 2 - a) [left] Melt chamber and necessary connections and b) [right] melt chamber in open position

the upper half in a fixed position. The lower tensile half is given approximately 2 mm of vertical freedom by loosening the lower grip in order to avoid the formation of any tensile stresses due to thermal contraction. The quartz crucible is placed on the shelf of the lower tensile half and a 0.5" diameter x 0.375" piece of filler metal is placed in the top of the crucible. This filler material is machined from the same metal as the tensile specimen. The filler metal is necessary to ensure complete filling of the crucible on melting.
The samples are positioned within 2 mm of one another and then the heating chamber is closed.
The optical pyrometer is positioned by using the laser dot sight which is aimed at the sample. The access port of the heating chamber is plugged and argon is purged for 10 minutes prior to heating the sample.
The sample is rapidly heated above the liquidus and the lower crosshead is raised until the liquid metal fills the melt crucible completely. The upper argon inlet is then closed to force the heat extraction mainly in the downward direction and allow the solidification front to move upward.
This prevents the shrinkage cavity from forming within the deformation zone. The power input to the induction coil is manually decreased so as to achieve a cooling rate of approximately 0.05˚C/sec through solidification. The lower crosshead is incrementally raised in order to maintain a light compression on the sample and avoid formation of unwanted voids. The temperature value during this solidification step can only be treated as qualitative data due to the presence of the quartz crucible.
On reaching a temperature reading of 1300˚C the upper argon inlet is turned on to avoid overheating of the upper tensile grips. On reaching a temperature reading of 1250˚C, the power is turned off completely and the crucible is broken away from the solidified tensile sample via the access port. The process of removing the crucible, from power off to power on, takes less than 30 seconds. The temperature drop during this time is severe, approximately 200˚C. However, because of the sample remaining in the austenitic range and the sluggish precipitation kinetics of AlN in austenite, it is reasonable to assume that this brief low temperature period has little or no effect on the results.
Once the heating power has been switched back on, the pyrometer is adjusted to give the maximum (true) temperature reading. The induction coil control is immediately switched to automatic mode and the closed-loop control follows the desired thermal path. On reaching the testing temperature, the power input to the induction coil is set as constant to avoid potential fluctuations during the deformation. The load cell and displacement sensor are zeroed and then tension is applied to the sample at a constant lower cross-head speed of 0.005 inches/second until failure occurs.
Immediately after failure occurs, the induction coil power is turned off and the sample is quenched via a high-velocity helium jet.
Three basic thermal paths were followed after solidification:

- Direct cool to varied tension testing temperature
- Undercool to varied temperature, reheat to 1000°C, tension test
- Undercool to 900°C, hold for varied time, reheat to 1000°C, tension test

The P20 materials with varied aluminum and nitrogen contents were tested under each of the thermal paths while the 3.5Ni and 4130 materials were tested only with the direct cooling path for comparison to the P20-mid material.

RESULTS

Ductility results for the experiments performed are presented below in the form of percent reduction of area versus temperature. The reduction of area was measured using the final fracture cross-section in comparison to the as-solidified minimum cross-section of 9.8 mm diameter.

DIRECT COOL TEST TEMPERATURE

The samples which were cooled directly to the testing temperature are intended to provide information about the ductility of the as-cast ingot during the solidification and cooling period while in the ingot mold and shortly after removing the ingot from the mold. Figure 3 shows the thermal path for the direct cool to test temperature experiments. Figure 4 shows the results as %reduction of area vs testing temperature for the P20 materials and Figure 5 shows the results for varied base compositions (P20, 3.5Ni, 4130).

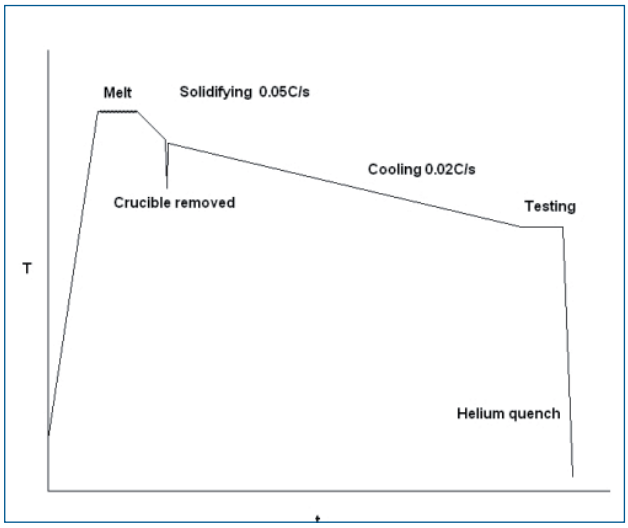

Fig. 3 - Thermal path for direct cooling to test temperature experiments

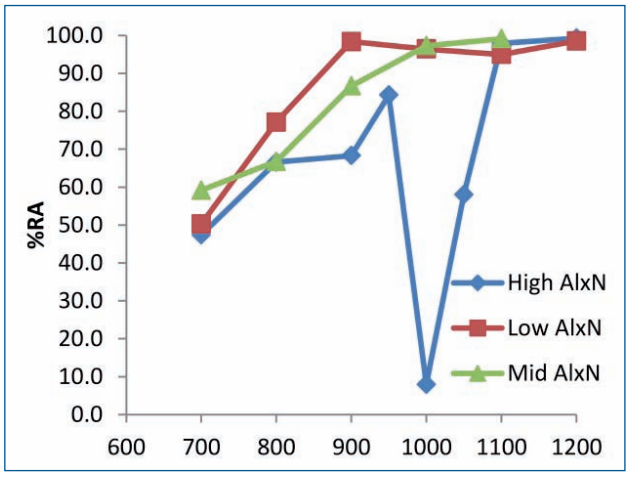

Fig. 4 - Results of direct cooling to test temperature experiments for P20 with varied aluminum and nitrogen

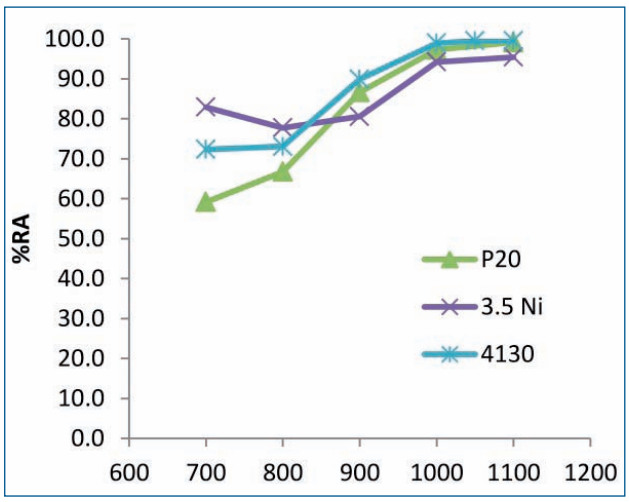

Fig. 5 - Results of direct cooling to test temperature experiments for varied base compositions

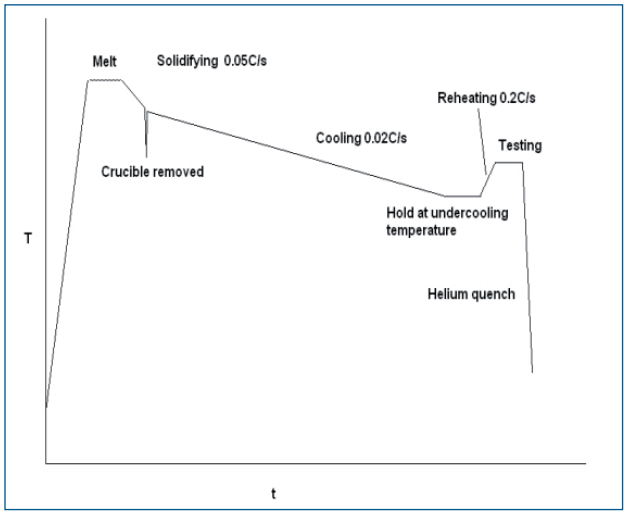

Fig. 6 - Thermal path for undercooling experiments

UNDERCOOL TO VARIED TEMPERATURE

The undercooling experiments are intended to provide information on the ductility of an as-cast ingot which is being heated to forging temperatures or is thermally insulated on the surface after the initial cool down. The varied undercooling temperatures would correspond to different "track times" that may be experienced in industry. For these tests, the samples were melted and then cooled at 0.02 °C/s to the desired undercooling temperature, held for 240 seconds at the undercooling temperature and then reheated at 0.2 °C/s to 1000 °C and tested. The value of 300 °C for the lowest temperature samples is for representation purposes only. The actual temperature was not measured but the sample was allowed to fully transform. Full transformation was ensured by monitoring the load cell readout; heating to 1000 °C was not started until 10 minutes at constant load was achieved. Figure 6 shows the undercooling thermal path, and the results of the experiments are shown in Figure 7. The samples with an undercooling temperature of 1000 °C are the direct cooling experiment results and are shown for comparison.

UNDERCOOL TO 900°C WITH VARIED HOLD TIME

The poor ductility of the mid- and low-AlxN samples for the testing described in the previous section prompted further investigation. Samples were tested at 1000 °C after various hold times at 900 °C in order to examine the change in ductility as a function of hold time. The thermal path is the same as shown in Figure 6 and the results are presented in Figure 8 with %RA as a function of hold time at 900 °C.

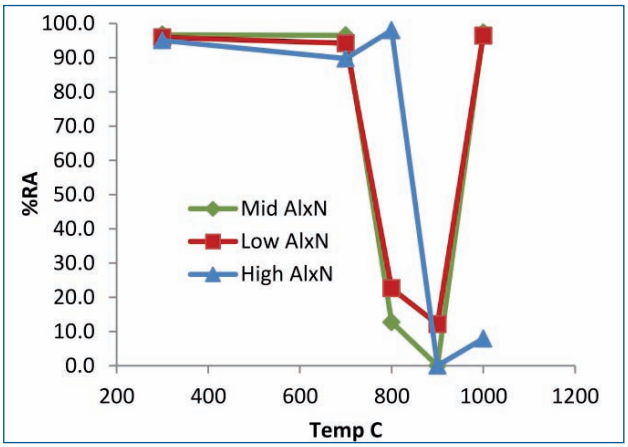

Fig. 7 - Results of undercooling experiments

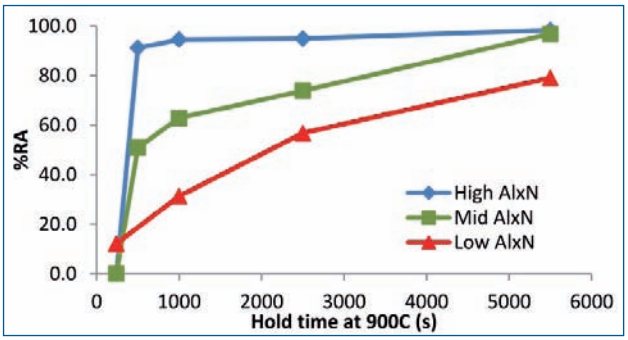

Fig. 8 - Results of undercooling experiments with varied hold times at 900 °C

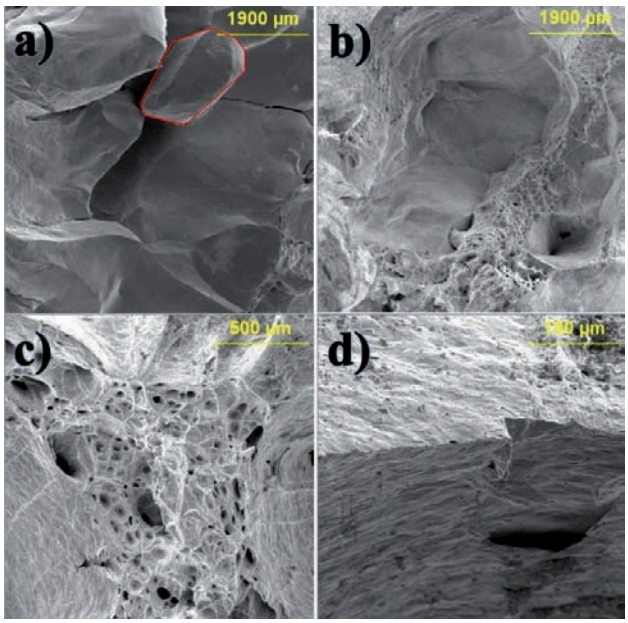

Fig. 9 - SEM images of a) intergranular, b) mixed mode, c) microvoid coalescence and d) fully ductile failures

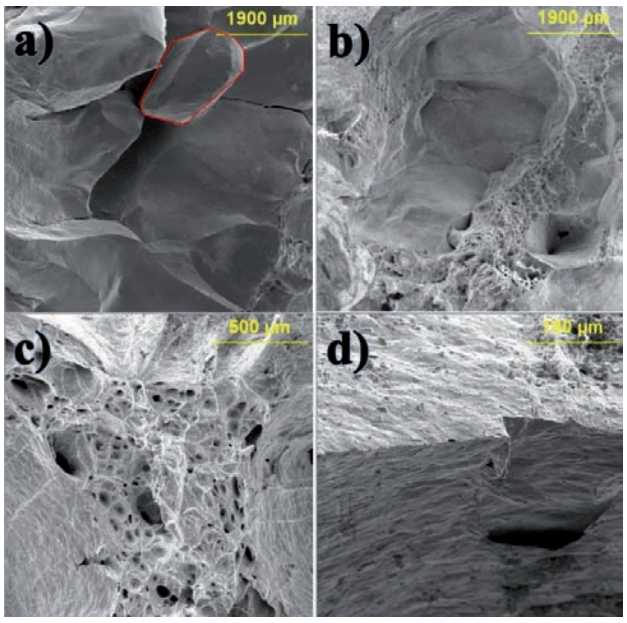

Fig. 10 - SEM-EDS analysis showing a) low magnification view of intergranular crack, b) higher magnification view of intergranular crack, c) EDS analysis of matrix material and d) EDS analysis of segregated second phase

METALLURGICAL ANALYSIS

The fracture surfaces of the tensile specimens were completely intergranular for samples that exhibited less than 20% RA. One such fracture is shown in Figure 9a. The highlighted grain in Figure 9a was mechanically removed for further analysis. Samples with 20% - 60% RA showed a mixed fracture mode of intergranular failure and microvoid coalescence as shown in Figure 9b.

Samples with greater than 60% RA failed mainly by microvoid coalescence with occasional, small areas of intergranular separation. A typical fracture face showing microvoid coalescence is shown in Figure 9c. Samples with near 100% RA do not contain enough fracture surface for analysis due to the necking of the sample down to a single point or line as shown in Figure 9d.

Grain boundary separation is visible on the fracture face shown in Figure 9a. At higher magnifications, a thin film containing additional microcracks along this grain boundary was visible.

EDS analysis showed a second phase of heavily segregated composition (increased phosphorus and sufur) near the separated grain boundary. Figures 10a through 10d show progressively higher magnification and EDS analysis of this area. The segregated phosphorus and sulfur are apparent.

As noted earlier, the highlighted grain in figure 9a was mechanically removed in order to examine the facets not exposed to any atmosphere during testing. Even with the

argon atmosphere during testing, the high temperature and long testing time allows for some very mild oxidation of the sample fracture surface. Figure 11 shows the grain surface below the fracture cross-section after it was removed. The dendritic structure and a thin grain boundary film are readily visible. The transition between the grain surface and the grain boundary film is highlighted in the lower right of the figure.
Many non-metallic inclusions were found on the surface of this grain, including MnS, Mn/CuS and V(C,N). Typically the MnS inclusions were quite large, on the order of 5 – 10 µm. The Mn/CuS particles were smaller (1 - 5 µm) and less frequent. The vanadium carbonitride particles were dispersed all over the grain surface and were much smaller than the sulfide precipitates, typically all much less than 1 µm as can be seen in Figure 12. Brown et. al.[4] have shown that V(C,N) precipitates form preferentially over AlN at intermediate temperatures and their presence should be expected even with the greater solubility limit of V(C,N). This is likely due to the high misfit strain of the hexagonal close-packed aluminum nitride particles compared to the cubic V(C,N) precipitates.

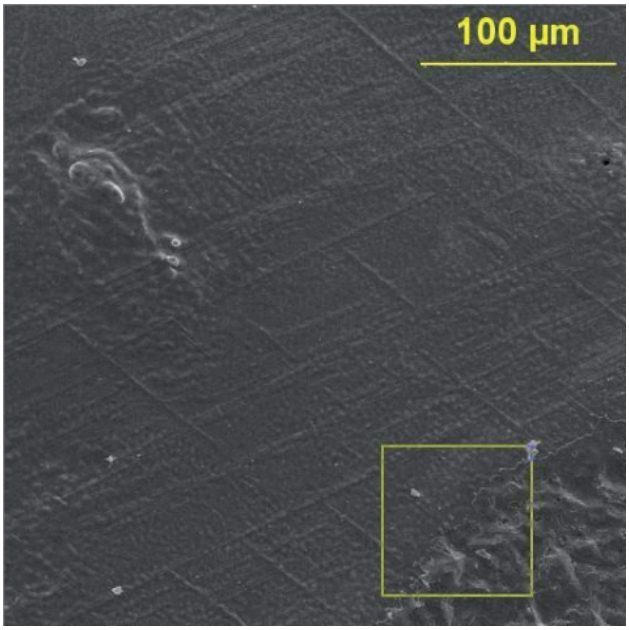

Fig. 11 - SEM image showing dendritic fracture surface with thin film

DISCUSSION

From the fracture surfaces shown, it is obvious that poor ductility is resultant from some form of grain boundary weakening or embrittlement. Within the P20 material samples, the only significant variation in composition is that of aluminum and nitrogen contents. This implies that the different behaviors of the P20 materials can only be due to formation of aluminum nitride particles or the effects of aluminum and nitrogen in solution. The variation in aluminum and nitrogen content is significant with respect to the solubility product of AlN (variation of over an order of magnitude), while only subtle differences, if any, would be expected from solid solution effects.
The direct cooling to test temperature experiments showed results that were in reasonable agreement with similar works. The P20-high AlxN product material shows a significant drop in ductility at temperatures between 950°C and 1050°C. This temperature range is consistent with the onset of aluminum nitride precipitation according to several published solubility products. There is essentially no ductility loss in the intermediate AlxN product material until below 900°C and no ductility loss in the low AlxN product material until below 800°C.
Perhaps the most interesting results of this work are the improved ductility of high AlxN material in the undercooling experiments as compared to the low- and mid-AlxN materials. All samples showed that improved ductility occurs at undercooling to temperatures of 700°C and below, but the high-AlxN material showed excellent ductility even at 800°C. With extended holding times at the undercooling temperature of 900°C, the rate of ductility recovery increases with increasing AlxN product. The cause for this improved ductility in the high AlxN material is thought to be due to aluminum nitride particle coarsening. For a given volume fraction of grain boundary precipitate, the pinning force is inversely related to the radius of the precipitates. The extremely hyperstoichiometric composition of the high-AlxN material can be expected to undergo particle coarsening at a much faster rate than in the mid- or low-AlxN P20 material, which would explain the faster increase in ductility. The mid- and low-AlxN P20 materials did not exhibit poor ductility on direct cooling to 900°C or 1000°C, but on undercooling to 900°C and reheating to the test temperature of 1000°C both materials showed essentially zero ductility. It has been noted [1,7,8,9] that precipitation of aluminum nitride is very rapid upon reheating samples that have been previously cooled to a lower temperature. The reason for this is not perfectly clear, however it is likely that the reduced incubation time for AlN precipitation at lower temperatures allows for a significant amount of precipitation to occur during the undercooling step while the decreased temperature prevents rapid growth. Upon undercooling, a significant amount of nuclei can form and growth occurs during the reheating period, whereas in the direct cooling of these samples the volume fraction of precipitates at the time of testing remains low.
The full recovery of ductility that occurs on undercooling to low temperatures is a result of a significant volume fraction of ferrite precipitation. On re-austenitizing, the harmful precipitates and segregated compositions that were present on the prior austenite grain boundaries become dispersed throughout the newly formed austenite grains.
The differences with varying base composition were very subtle. This work has shown that increasing the nickel content causes a small decrease in ductility at temperatures above 850°C while there is a slight increase in ductility at temperatures below 850°C. Erasmus[10]

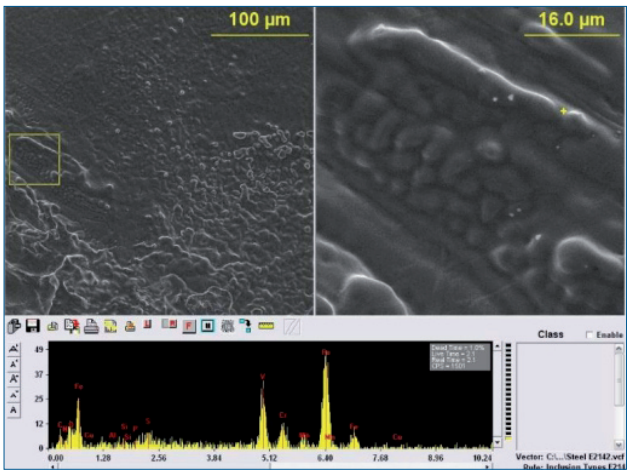

Fig. 12 - Showing EDS analysis of V(C,N) precipitate

noted that additions of nickel decrease the solubility of nitrogen in austenite which will raise the precipitation temperature of aluminum nitride. However, in examining the Fe-N-Ni system[11] it is seen that the effect is minimal. For example at 1200°C, an increase from 0.0% Ni to 3.3% Ni only decreases the soluble nitrogen from 235 ppm down to 210 ppm.

SUMMARY

There is very little published information available regarding the hot ductility of large-grained, as-cast, slow-cooled steels. A thorough understanding of the effects of thermal path and composition on ductility can provide ingot producers and forgers with the fundamental information necessary for well-designed thermal handling and processing procedures. The following important points are noted from this work:

Ingot handling within the temperature range of 950°C - 1050°C should be avoided for materials with high aluminum and nitrogen contents.

Poor ductility may be experienced in cast steels even with relatively low aluminum and nitrogen contents in cases where temperature oscillations occur in the temperature range of 900°C - 1000°C.

Hyperstoichiometric AlxN compositions can show rapid recovery of ductility during holding at high temperature, however in EAF steels the necessary aluminum content will likely cause precipitation problems at higher temperatures.

As-cast, slowly cooled steels exhibit severe austenite grain boundary segregation of phosphorus and sulfur as well as grain boundary precipitation of sulfides and carbonitrides.

Aluminum nitride is also expected on the austenitic grain boundaries but its presence was not confirmed in this work.

The effect of increased nickel content was found to be mild in this work. At higher temperatures the ductility is slightly reduced with increasing nickel and at lower temperatures the ductility is slightly improved.

It must be noted that the work described in this paper is ongoing. A deeper understanding of themechanisms of ductility loss in the experiments presented here will be gained via TEM analysis of thin foil and carbon extraction replicas from the samples along with additional metallographic examination.

REFERENCES

1) F.G. Wilson and T. Gladman, “Aluminum nitride in steel”, International Materials Reviews, 1988, Vol. 33, No. 5, 221 – 283.
2) T. Revaux, J.P. Bricout and J. Oudin, “A New Tensile Testing Procedure for Predicting Transverse Cracking Susceptibility of Continuous Casting Slabs”, Journal of Materials Engineering and Performance, April 1996, Vol. 5(2), 260 – 268.
3) W.T. Nachtrab, W.T. and Y.T. Chou, “The Effect of Sn, Al, and N on the Hot Ductility of a Carbon-Manganese Steel between 700˚ and 1200˚C”, Metallurgical Transactions A, May 1988, Vol. 19A, 1305 – 1309.
4) E.L. Brown, L.J. Cuddy and A.J. DeArdo,”Aluminum Nitride Precipitation in Microalloyed Steels”, The Thermomechanical Processing of Microalloyed Austenite, A.J. DeArdo, G.A. Ratz and P.J. Wray, Editors, (Warrendale, PA, TMS-AIME: 1982), 319 – 341.
5) M. Vedani, D.Dellasega and A. Mannuccii, “Characterization of Grain-boundary Precipitates after Hot-ductility Test of Microalloyed Steels”, ISIJ International, 2009, Vol. 49, No. 3, 446 – 452.
6) A. Nicholson, “Hot Workability Testing of Steels”, Iron & Steel, June - July 1964, 290 – 294, 363 – 380.
7) U.H. Lee, T.E. Park, K.S. Son, M.S Kang, Y.M. Won, C.H. Yim, S.K Lee, I. Kim, and D. Kim, “Assessment of Hot Ductility with Various Thermal Histories as an Alternative Method of in situ Solidification”, ISIJ International, 2010, Vol. 50, No. 4, 540 – 545.
8) G.A. Wilber, R. Batra, W.F. Savage and W.J Childs, “The Effects of Thermal History and Composition on the Hot Ductility of Low Carbon Steels”, Metallurgical Transactions A, September 1975, Vol. 6A, 1727 – 1735.
9) C. Spradbery and B. Mintz, “Influence of undercooling thermal cycle on hot ductility of C-Mn-Al-Ti and C-Mn-Al-Nb-Ti steels”, Iron and Steelmaking, 2005, Vol. 32, No. 4, 319 – 324.
10) L.A. Erasmus, “Effect of aluminum additions on forgeability, austenite grain coarsening temperature, and impact properties of steel”, Journal of the Iron and Steel Institute, January 1964, 32 – 41. [correspondence from Dec 1964 included].
11) P. Perrot, “Iron-Nitrogen-Nickel”, MSIT, Springer Material Database, 2008.